Energy Proceedings
Vol 55, 2025
ISSN 2004-2965

Performance analysis of fuel cell hybrid-electric regional aircraft based on hydrogen/helium co-cooling#

Mingliang Bai[1], Wenjiang Yang[1,2*], Zibing Qu[1], Ruopu Zhang[1], Juzhuang Yan[1]

1 School of Astronautics, Beihang University, Beijing 100191, China

2 Aircraft and Propulsion Laboratory, Ningbo Institute of Technology, Beihang University, 315100, China

(Corresponding Author: yangwjbuaa@buaa.edu.cn)

ABSTRACT

This paper presents a fuel cell hybrid electric propulsion system (FCHEPS) that integrates hydrogen fuel cell, cryogenic cooling, and superconducting technology, specifically designed for modern twin-engine turboprop regional aircraft. A parametric modeling approach was applied to key components, including hydrogen fuel cells, superconducting motors, and liquid hydrogen tanks. Additionally, a micro-channel plate hydrogen-helium heat exchanger (HX) was developed to maintain the optimal inlet temperature for the fuel cell and to cool cryogenic components. Energy management strategies based on state machine (SM) and equivalent consumption minimization strategy (ECMS) were developed to achieve optimal power distribution. Simulation results across cruise and emergency mission profiles validated the effectiveness of the powertrain configuration, analysis model and energy management strategies. The ECMS method demonstrated minimal fuel consumption and maximum energy conversion efficiency, making it particularly suitable for scenarios with frequent power demand fluctuations.

Keywords: fuel cell, heat exchanger, hybrid electric propulsion system, liquid hydrogen cooling, superconducting motor, thermal management

NONMENCLATURE

Abbreviations	
ECMS	Equivalent consumption minimization strategy
EMS	Energy management strategy
FCHEPS	Fuel cell hybrid electric propulsion system
HEPS	Hybrid electric propulsion system
HX	Heat exchanger
HTS	High-temperature superconducting
SCM	Superconducting motor
SM	State machine
TMS	Thermal management system
PMAD	Power management and distribution
PTW	Power-to-weight

1. INTRODUCTION

Under the guidance of policies such as the N+3, Flightpath 2050 and Waypoint 2050, the aviation industry urgently needs to develop new power system architectures and improve energy efficiency to achieve sustainable development [1]-[2]. High power and electrification are the inevitable trend of the power systems development. However, the current technological level of electrical components fails to meet the expected efficiency and power-to-weight (PTW) requirements [3].

Superconducting technology and cryogenic cooling technology are key solutions to enhancing the performance of electrical components, with superconducting components demonstrating significant advantages in PTW ratio and efficiency. Considering sustainable energy supply, the specific energy of hydrogen fuel is three times that of aviation kerosene and 60 times that of battery, indicating that loading the same mass of hydrogen fuel can significantly improve aircraft performance [4]. Hydrogen energy can be used for turbine combustion, fuel cell power generation, and cryogenic cooling, and its environmental friendliness, renewability, and cooling performance make it the optimal energy choice. Liquid hydrogen (LH_2) is suitable for cooling onboard superconducting materials and electrical components, while gas hydrogen (GH_2) can be used as fuel for fuel cells, thereby enabling the recycling of hydrogen energy in onboard systems [4][5].

This is a paper for the 16th International Conference on Applied Energy (ICAE2024), Sep. 1-5, 2024, Niigata, Japan.

The fuel cell hybrid electric propulsion system (FCHEPS) uses hydrogen as both fuel and cooling medium. Hydrogen fuel cells and energy storage units work together to generate electricity, driving superconducting motors to propel the aircraft. FCHEPS offers advantages such as high energy efficiency, multi-energy source synergy, and environmental friendliness, providing flexible power output to adapt to various operating conditions and save energy. Based on the current development level of system components, FCHEPS is primarily suitable for commuter [6], small regional [7], and single-aisle aircraft [8][9]. However, few studies have focused on the integrated energy management of FCHEPS, the application of hydrogen-helium heat exchangers for thermal management of cryogenic components, and the design of effective energy management strategies (EMSs) to achieve efficient matching of multiple power sources.

This paper presents the design of a FCHEPS configuration utilizing hydrogen-helium cooperative cooling. Through the development of analytical models, the design of cooling circuits, and the formulation of power matching strategies, this study conducts a comparative analysis under two distinct flight profiles. The findings offer a theoretical foundation for the design and control of megawatt-class hydrogen-electric aircraft.

2. FUEL CELL HYBRID ELECTRIC PROPULSION SYSTEM

2.1 Hybrid-electric aircraft configuration

A regional hybrid-electric aircraft, retrofitted from a twin-engine turboprop, features a liquid hydrogen (LH_2) tank positioned in the aft fuselage and a battery pack located in the lower fuselage. The original engine nacelles on either wing have been replaced with primary power units, each comprising a hydrogen fuel cell, DC/AC inverter, superconducting motor, and propeller.

The powertrain configuration of the hybrid-electric aircraft is illustrated in *Fig. 1*. LH2 flows from the hydrogen distribution unit (HDU) to the hydrogen-helium heat exchangers (HX) on both sides, enabling helium circulation to cool high-temperature superconducting (HTS) cables and superconducting motors (SCMs) along with their controllers. Simultaneously, gaseous hydrogen (GH_2) is supplied to the fuel cell system through pipelines, with temperature, pressure, and flow rate regulation at the anode. The battery is connected to the 1000 V high-voltage bus via a DC/DC converter, enabling peak shaving and valley filling through the power management and distribution (PMAD) unit. A supercapacitor is employed to maintain bus voltage stability and manage high currents during load power fluctuations.

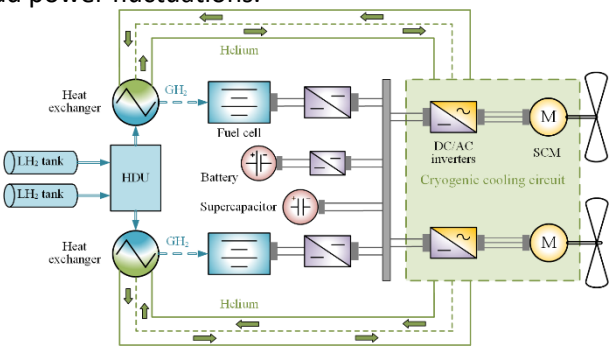

Fig. 1 Powertrain configuration of a fuel cell hybrid electric aircraft

2.2 Mission power requirements

The mission profiles for the fuel cell hybrid electric aircraft include a typical cruise flight with smooth power demand changes and a emergency mission flight with significant power demand fluctuations. The former has a flight duration of 5400 seconds, with a maximum power demand of 1.5 MW during the first climb and 1 MW during the second climb. The latter profile describes complex power variations under emergency conditions, with a flight duration of 350 seconds and power demand fluctuating between 0 and 2 MW.

2.3 Components modeling

This study focuses on the detailed modeling of the fuel cell hybrid electric propulsion system (FCHEPS), including key components such as the hydrogen fuel cell, superconducting motor, liquid hydrogen (LH2) tank, hydrogen-helium heat exchanger, and other critical elements.

2.3.1 Hydrogen fuel cell

The hydrogen fuel cell system configuration, as illustrated in *Fig.* , includes the cathode air supply, anode hydrogen recirculation system, fuel cell stack, cooling system and control units.

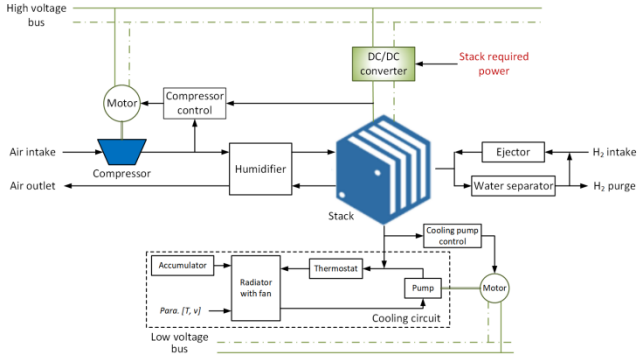

Fig. 2 Detailed model of hydrogen fuel cell[10]

In the cathode air supply system, air enters the compressor through the air intake. Before reaching the stack, the air passes through a membrane humidifier, which maintains the moisture of the membrane to enhance electrochemical reaction efficiency. A high-voltage motor drives the compressor via a reduction gear, and the compressor control unit calculates the motor's input torque based on air flow rate, oxygen flow rate, and current to ensure that the oxygen stoichiometry is maintained.

In the anode hydrogen recirculation system, an ejector supplies hydrogen at the appropriate temperature, pressure, and flow rate to the stack, ensuring a continuous supply of hydrogen. A functional water separator removes water produced by the fuel cell reaction, preventing water accumulation on the anode side. Inside the stack, hydrogen and oxygen undergo an electrochemical reaction, producing electrical energy, water, and heat. The generated direct current is converted and regulated by a DC/DC converter before being delivered to the high-voltage bus. The input current to the DC/DC converter is determined by the ratio of the required power ($P_{req,fc}$) to the bus voltage.

A cooling pump circulates the coolant to remove heat generated by the stack. A low-voltage motor directly drives the pump, and a PI controller calculates the motor input torque by processing the temperature difference between the stack and the target temperature. The thermostat regulates the coolant flow based on preset temperature thresholds. If the coolant temperature exceeds the threshold, it is directed to the radiator, which enhances heat dissipation by increasing the contact area between the coolant and ambient air. If cooling demand rises further, a fan is activated to facilitate forced air convection for more efficient cooling.

The parametric modeling data for the hydrogen fuel cell can be referenced from sources [7] and [10]. Based on the required stack power and polarization curves, parameters such as effective area, anode hydrogen flow rate, cathode air flow rate, stack heat dissipation, and component mass can be calculated.

2.3.2 Superconducting motor

The superconducting motors adopt a rotor semi-superconducting topology, using ReBCO HTS material to replace conventional rotor material. Cold helium is utilized as a cryogenic cooling medium to maintain the superconducting material below its critical temperature, ensuring its superconducting properties. The peak design power of the SCMs is 1 MW, directly driving the aft propeller. The power-to-weight ratio can be calculated using the following equation:

$$PTW_{scm} = \frac{\pi}{30}\omega_{scm} \cdot TTW_{scm} \cdot 10^{-3} \tag{1}$$

where ω_{scm} is the speed of SCM, TTW_{scm} represents the torque-to-weight ratio. The efficiency of the SCM is specifically represented by cold-end efficiency and warm-end efficiency. The heat loss generated at the cold end is removed by the cryogenic cooling circuit, while the heat loss generated at the warm end is rejected by the thermal management system.

$$\begin{aligned} \eta_{scm} &= \frac{1}{\frac{1}{\eta_{scm,c}} + \frac{1}{\eta_{scm,w}} - 1} \\ \dot{Q}_{scm,c} &= P_{scm} \cdot (1 - \eta_{scm,c}) \\ \dot{Q}_{scm,w} &= P_{scm} \cdot (1 - \eta_{scm,w}) \end{aligned} \tag{2}$$

The mass and losses of the cryogenic DC/AC inverter are determined based on the power density, apparent power, and power factor of the SCM. Additionally, the inverter input must account for the extra losses caused by reactive currents, which leads to the actual efficiency being lower than the rated efficiency.

$$\begin{aligned} M_{inv} &= \frac{P_{scm}}{PF_{scm} \cdot PTW_{inv}} \\ \dot{Q}_{inv} &= \frac{P_{scm}}{PF_{scm}} \cdot (\frac{1}{\eta_{inv}} - 1) \\ \eta_{inv,in} &= \frac{PF_{scm}}{\frac{1}{\eta_{inv}} - 1 + PF_{scm}} \end{aligned} \tag{3}$$

2.3.3 Liquid hydrogen tank

A LH_2 tank with hemispherical ends and cylindrical body is selected, using aluminum alloy 2219 for the tank walls and polyurethane foam as the insulation material [10][11]. The modeling of tank dimensions considers geometric design, mechanical design and thermal design. The geometric dimensions are determined by the aircraft volume capacity and fuel tank dimensions. The mechanical design involves calculating the tank wall thickness based on the radius, the tank wall material stress coefficient, and a safety factor. Thermal design involves calculating the surface temperature of insulation material based on heat balance and determining the insulation thickness by considering evaporation rate, thermal conductivity and tank length.

The gravimetric efficiency of the tank is defined as the ratio of the stored LH_2 mass to the total mass.

$$\eta_{tank} = \frac{M_{LH2}}{M_{LH2} + M_{tank}} \tag{4}$$

2.3.4 Hydrogen-helium heat exchanger

The hydrogen-helium heat exchanger (HX) described in this paper employs a micro-channel plate structure, consisting of multiple layers of thin metal plates etched with micro-channels[12]. As shown in *Fig. 3*, heat exchange between hydrogen and helium occurs through convection and conduction within these micro-channels, providing a large surface area and highly efficient heat transfer performance. Helium flows through a set of micro-channels, transferring heat to the plates. The plates then conduct this heat to the hydrogen flowing through an alternate set of micro-channels, where hydrogen absorbs the heat, completing the heat exchange process. The plates are made of austenitic stainless steel and are brazed together, forming a robust and compact structure[12].

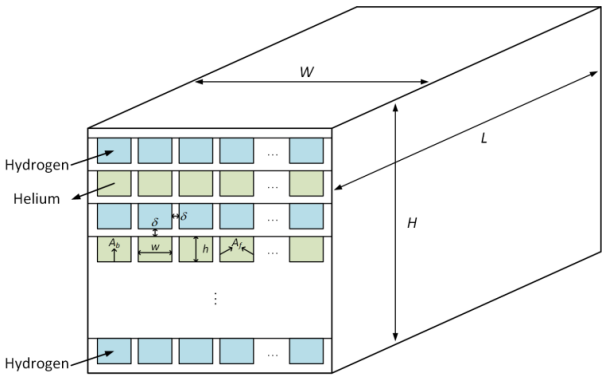

Fig. 3 Structure of micro-channel plate heat exchanger

Heat transfer within the HX consists of three components: convective heat transfer between helium and the wall surface, conductive heat transfer through the wall, and convective heat transfer between the wall surface and hydrogen. According to the first law of thermodynamics, the heat flux balance can be expressed as:

$$Q = (C(T_{in} - T_{out}))_{He} = (C(T_{out} - T_{in}))_H \\ C_j = (\dot{m} \cdot c_p)_j, j = He / H \quad (5)$$

where Q is the heat flux, T_{in} and T_{out} represents the inlet and outlet temperature, C is the heat capacity, c_p is specific heat capacity. In addition, heat flux can be calculated as:

$$Q = U_j \cdot A_j \cdot \Delta T_{ave} \quad (6)$$

$$\Delta T_{ave} = \frac{\Delta T_{\max} - \Delta T_{\min}}{\ln \frac{\Delta T_{\max}}{\Delta T_{\min}}}$$

$$\Delta T_{\max} = \max\{T_{He,in} - T_{H,out}; T_{He,out} - T_{H,in}\} \quad (7)$$

$$\Delta T_{\min} = \min\{T_{He,in} - T_{H,out}; T_{He,out} - T_{H,in}\}$$

where U_j represents heat transfer coefficient, A_j is the heat transfer aera, ΔT_{ave} represents logarithmic mean temperature difference. The overall heat transfer coefficient U_j incorporates the thermal resistances of the helium side, the partition material and the hydrogen side, as illustrated in Equ. (8).

$$U_j = \frac{1}{\frac{A_j}{(\eta_t k A)_{He}} + \frac{t_p A_j}{\lambda_0 A_0} + \frac{A_j}{(\eta_t k A)_H}} \quad (8)$$

where t_p represents the plate thickness, k is the convective heat transfer coefficient, λ represents thermal conductivity. The overall efficiency η_t can be determined based on the fin efficiency, plate surface area and fin surface area, where the fin efficiency is derived from the geometric and material properties.

$$\eta_{t,j} = ((A_b + \eta_f A_f) / A_t)_j \\ A_t = A_b + A_f \quad (9) \\ \eta_f = \frac{tanh(\sqrt{\frac{2h}{\lambda t_f}}(h + \frac{t_f}{2}))}{\sqrt{\frac{2h}{\lambda t_f}}(h + \frac{t_f}{2})}$$

2.3.5 Other components modeling

The energy storage system consists of a battery pack and supercapacitors (SCs). The battery is modeled using an equivalent circuit approach, with high energy density $LiFePO_4$ cells selected. The number of cells in series and parallel configurations is determined based on the operating time, power and energy requirements. The variation in state of charge (SOC) is a key metric for assessing the effectiveness of the energy management strategy in terms of energy balance, cost and efficiency. Additionally, SCs are designed to stabilize the bus voltage and reduce the impact of large charging or discharging currents on the battery.

The high-temperature superconducting (HTS) cables use ReBCO superconducting material, known for its high current-carrying capacity and 99% transmission efficiency. The required cable length is calculated based on the aircraft layout and component connections, with the total mass determined by combining this length with specific mass parameters.

3. INTEGRATED ENERGY MANAGEMENT

The integrated energy management of the fuel cell hybrid electric propulsion system primarily involves two key aspects: thermal management and power distribution. Thermal management includes cryogenic cooling, heat exchange, and the thermal management

unit, all of which ensure the proper operation of components and minimize heat loss. Power management focuses on optimizing power distribution between the fuel cell and energy storage units during various flight phases, ensuring efficient and reliable propulsion.

3.1 Cryogenic cooling circuit

The cryogenic cooling circuit of the fuel cell hybrid electric propulsion system is illustrated in *Fig. 4*. The liquid hydrogen (LH_2) tank supplies LH_2 to the hydrogen-helium heat exchangers (HXs) on both sides via the distribution unit. The evaporated hydrogen then flows to the anode of the hydrogen fuel cell. Simultaneously, the cooled helium circulates to cool the high-temperature superconducting (HTS) cables, power electronics control unit, and superconducting motor. As the helium absorbs heat and its temperature rises, it returns to the hydrogen-helium HXs for cooling.

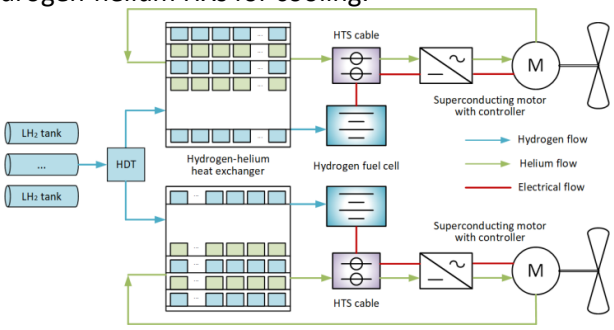

Fig. 4 Cryogenic cooling circuit of FCHEPS

3.2 Thermal management system

The thermal management system (TMS) of FCHEPS is designed to remove heat losses from non-cryogenic components, including fuel cell stack and exhaust heat loss, battery heat loss, battery-side DC/DC converter heat loss, and superconducting motor heat loss.

$$\dot{Q}_{TMS} = \dot{Q}_{fc,stack} + \dot{Q}_{fc,exh} + \dot{Q}_{bat} + \dot{Q}_{conv} + \dot{Q}_{scm,w} \quad (10)$$

This paper adopts a ram air-based thermal management system configuration, which features a simple structure and efficiently removes a large amount of heat per unit volume [7]. The ram air-based TMS utilizes the dynamic pressure generated by the aircraft's motion to draw air into the ducts, where it absorbs waste heat from the components through an air-air or air-liquid heat exchanger, before being expelled overboard. When the aircraft is stationary or operating at low speeds on the ground, an additional fan is employed to ensure sufficient air intake.

3.3 Power management and distribution

The power management and distribution unit (PMAD) is designed to balance power demand and supply, efficiently distributing output power from the fuel cell and battery via an energy management controller. This study utilizes two energy management strategies: a rule-based control state machine (SM) and an optimization-based equivalent consumption minimization strategy (ECMS). A comparative analysis of these strategies is conducted, focusing on key metrics such as hydrogen consumption, battery energy consumption, and overall efficiency.

3.3.1 State machine strategy

The SM divides the system operating states into several discrete states, each corresponding to specific operating modes and control rules. The basic formula can be expressed as:

$$SOC(t+1) = f(SOC(t), P_{fc}(t), P_{req}(t)) \quad (11)$$

where battery state of charge (*SOC*) represents the system state at time *t*, the fuel cell power (P_{fc}) represents the control input at time *t*, and the load demand power (P_{req}) represents the external disturbance at time *t*. According to the SM control rules, as shown in *Tab. 1*, fuel cell output power is determined based on the current state *SOC(t)*, the load power demand $P_{req}(t)$, and the predicted state at the next time step *SOC(t+1)*.

Tab. 1 Control rules of state machine strategy

Input		***Output***
$SOC>SOC_{max}$	$P_{req}<P_{fc,min}$	$P_{fc}=P_{fc,min}$
	$P_{fc,min}\le P_{req}\le P_{fc,max}$	$P_{fc}=P_{req}$
	$P_{req}>P_{fc,max}$	$P_{fc}=P_{fc,max}$
$SOC_{min}<SOC<SOC_{max}$	$P_{req}<P_{fc,opt}$	$P_{fc}=P_{fc,opt}$
	$P_{fc,opt}\le P_{req}\le P_{fc,max}$	$P_{fc}=P_{req}$
	$P_{req}>P_{fc,max}$	$P_{fc}=P_{fc,max}$
$SOC<SOC_{min}$	$P_{req}<P_{fc,max}$	$P_{fc}=P_{req}+P_{bat,min}$
	$P_{req}\ge P_{fc,max}$	$P_{fc}=P_{fc,max}$

where the maximum and minimum SOC are set at 0.9 and 0.5, $P_{fc,opt}$ is the theoretical optimal power of fuel cell, and $P_{bat,min}$ represents the battery charge power.

3.3.2 Equivalent consumption minimization strategy

The core concept of the optimization-based control in ECMS is to equate battery energy consumption to fuel consumption. This approach converts the global optimization problem of managing energy between the battery and fuel cell into a local optimization problem, with the goal of minimizing equivalent hydrogen consumption. The optimization objective function is expressed as:

$$J = [P_{fc}(t) + \alpha(t)\cdot P_{bat}(t)]\cdot \Delta t \quad (12)$$

where $\alpha(t)$ represents the penalty coefficient, Δt is the sampling time. The equality constraints and inequality constraints are shown in Equ. (8) and (9) respectively.

$$P_{req}(t) = P_{fc}(t) + P_{bat}(t)$$

$$\alpha(t) = 1 - 2\mu \frac{(SOC(t) - \frac{(SOC_{\max} + SOC_{\min})}{2})}{SOC_{\max} + SOC_{\min}} \quad (13)$$

$$P_{fc,\min} \le P_{fc} \le P_{fc,\max}$$

$$P_{bat,\min} \le P_{bat} \le P_{bat,\max} \quad (14)$$

$$0 \le \alpha \le 1$$

where μ is a constant used to adjust the influence of the equivalent factor.

4. RESULTS AND DISCUSSION

This section compares and analyzes the parameter matching and component temperature characteristics of the fuel cell hybrid electric propulsion system (FCHEPS) under two mission profiles and different energy management strategies. The analysis focuses on fuel consumption, battery state of charge (SOC), system efficiency, as well as power and voltage-current matching characteristics across various flight profiles.

4.1 Cruise flight profile

Under the cruise flight mission profile, power demand is relatively smooth, allowing sufficient response time for the fuel cell. The battery provides auxiliary power, achieving peak shaving and valley filling. As shown in Fig. 5 (a), the SM strategy effectively matches the demand curve, while the ECMS may exhibit power oscillations in this scenario. From *Fig. 5(b)* and *Tab. 2*, it can be concluded that ECMS relies less on the fuel cell's output, resulting in a 2% optimization in fuel consumption compared to SM. On the other hand, SM achieves a higher final SOC value, reducing battery maintenance costs, although this also leads to a decrease in power conversion efficiency.

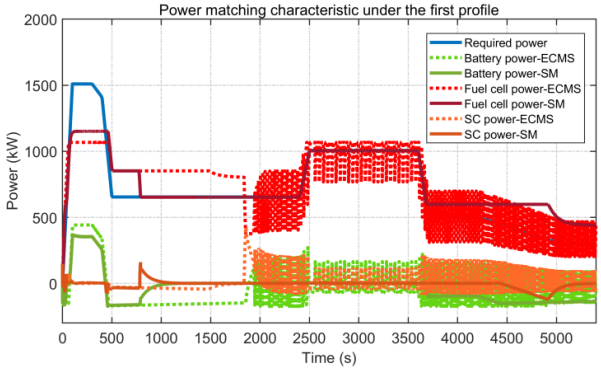

(a) power curve

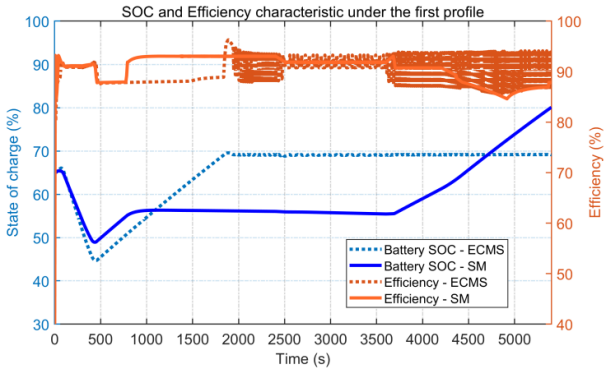

(b) SOC and efficiency

Fig. 5 Power, SOC and efficiency parameters of FCHEPS under the cruise mission profile

Tab. 2 Parameters comparison of FCHEPS under the emergency profile

Parameters	*SM*	*ECMS*	*Unit*
Hydrogen consumption	59.5	58.4	kg
Battery SOC final value	83	73	%
Maximum efficiency	91.7	95.8	%
Mean efficiency	84	87.6	%

4.2 Emergency flight profile

The emergency mission has a shorter flight duration but exhibits significant fluctuations in power demand over time. The power, voltage and efficiency characteristics of the FCHEPS are illustrated. The hydrogen fuel cell, despite its slow power response, serves as the primary power source. Battery and supercapacitor packs provide auxiliary power, with supercapacitors capable of handling high current surges to meet instantaneous load demands. When the power demand exceeds 1 MW, the power output of the hydrogen fuel cell under the ECMS strategy is slightly lower than that under the SM strategy. The supercapacitor effectively stabilizes the bus voltage. The voltages of the hydrogen fuel cell and lithium battery decrease as the power increases and show a slight increase as the power decreases, indicating that the DC/DC converters on both sides are operating normally.

The parameters of hydrogen consumption, battery SOC, and efficiency of the FCHEPS under this profile are summarized in the *Tab. 3*. Compared to the SM strategy, the ECMS effectively reduces fuel consumption, increases the final SOC value, and improves energy utilization efficiency.

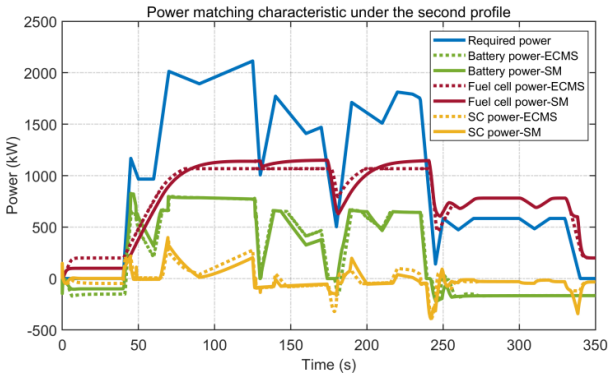

(a) power curve

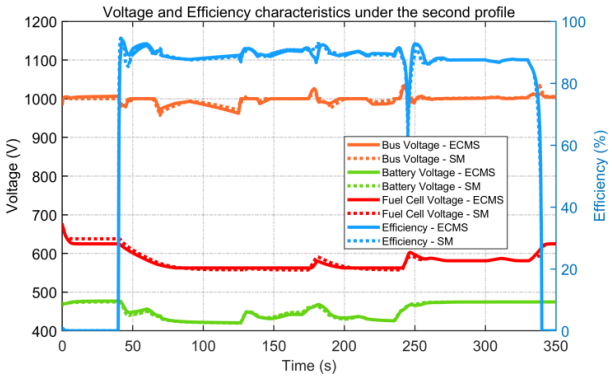

(b) voltage and efficiency

Fig. 6 Power, voltage and efficiency parameters of FCHEPS under the emergency mission profile

Tab. 3 Parameters comparison of FCHEPS under the emergency profile

Parameters	*SM*	*ECMS*	*Unit*
Hydrogen consumption	4.19	4.17	kg
Battery SOC final value	49.01	49.28	%
Maximum efficiency	94.6	94	%
Mean efficiency	85.5	85.8	%

5. CONCLUSIONS

This paper presents the design of a hydrogen-helium heat exchange-cooled fuel cell hybrid power system for regional aircraft. Key component models, including the hydrogen fuel cell, superconducting motor, liquid hydrogen storage tank, and hydrogen-helium heat exchanger, were developed. A cryogenic cooling circuit was designed to dissipate heat from various components, while two power control strategies were implemented to optimize the power source matching. Simulation results validated the effectiveness of the FCHEPS configuration, analytical models, and cryogenic cooling circuit. Compared to the rule-based SM strategy, the optimized ECMS strategy demonstrated lower fuel consumption, reduced battery power usage, and higher power conversion efficiency, especially under conditions of frequent power demand fluctuations.

REFERENCE

[1] Chao H, Agusdinata D B, DeLaurentis D, et al. Car-bon offsetting and reduction scheme with sustainable aviation fuel options: Fleet-level carbon emissions impacts for US airlines[J]. Transportation Research Part D: Transport and Environment, 2019, 75: 42-56.

[2] Krein A, Williams G. Flightpath 2050: Europe's vision for aeronautics[M]//Innovation for Sustainable Aviaition in a Global Environment. IOS Press, 2012: 63-71.

[3] Da Silva F F, Fernandes J F P, Da Costa Branco P J. Barriers and challenges going from conventional to cryogenic superconducting propulsion for hybrid and all-electric aircrafts[J]. Energies, 2021, 14(21): 6861.

[4] Nøland J K, Mellerud R, Hartmann C. Next-generation cryo-electric hydrogen-powered aviation: A disruptive superconducting propulsion system cooled by onboard cryogenic fuels[J]. IEEE Industrial Electronics Magazine, 2022, 16(4): 6-15.

[5] Nøland J K. Hydrogen Electric Airplanes: A disruptive technological path to clean up the aviation sec-tor[J]. IEEE Electrification Magazine, 2021, 9(1): 92-102.

[6] Tiwari S, Pekris M J, Doherty J J. A review of liquid hydrogen aircraft and propulsion technologies[J]. In-ternational Journal of Hydrogen Energy, 2024, 57: 1174-1196.

[7] Hartmann C, Nøland J K, Nilssen R, et al. Dual use of liquid hydrogen in a next-generation PEMFC-powered regional aircraft with superconducting pro-pulsion[J]. IEEE Transactions on Transportation Electrification, 2022, 8(4): 4760-4778.

[8] Waddington E, Merret J M, Ansell P J. Impact of liquid-hydrogen fuel-cell electric propulsion on aircraft configuration and integration[J]. Journal of Aircraft, 2023, 60(5): 1588-1600.

[9] Nam G D, Sung H J, Ha D W, et al. Design and anal-ysis of cryogenic cooling system for electric propulsion system using liquid hydrogen[J]. Energies, 2023, 16(1): 527.

[10] Bai M, Yang W, Yan J, et al. Cryogenic turbo-electric hybrid propulsion system with liquid hydrogen cooling for a regional aircraft[J]. International Journal of Hydrogen Energy, 2024, 71: 541-561.

[11] Boll M, Corduan M, Biser S, et al. A holistic system approach for short range passenger aircraft with cryogenic propulsion system[J]. Superconductor Science and Technology, 2020, 33(4): 044014.

[12] Pan X, Zhang S, Jiang Y, et al. Key parameters effects and design on performances of hydrogen/helium heat exchanger for SABRE[J]. International Journal of Hydrogen Energy, 2017, 42(34): 21976-21989.